Filtration membranes of reduced graphene oxide for dye removal – production and characterization

Andreza Menezes Lima[a,*], Anthony Matheus de Oliveira[a], Talita Gama de Sousa[a], Artur Camposo Pereira[a], Roberto Bentes de Carvalho[b], Wagner Anacleto Pinheiro[a]

[a]*Instituto Militar de Engenharia (IME), Seção de Engenharia de Materiais, Praça General Tibúrcio, 80 – Urca, Rio de Janeiro, Brasil, Tel. (21) 2546-7283; emails: andrezamenezeslima@gmail.com (A.M. Lima), anthonymatheuss@gmail.com (A.M. Oliveira), talitagama@gmail.com (T.G. Sousa), camposo.artur@gmail.com (A.C. Pereira), anacleto@ime.eb.br (W.A. Pinheiro)*
[b]*Pontifícia Universidade Católica do Rio de Janeiro (PUC-Rio), Departamento de Engenharia Química e de Materiais, Rua Marquês de São Vicente, 225 – Gávea, Rio de Janeiro, Brasil, email: rbcarvalho@puc-rio.br (R.B. Carvalho)*

ABSTRACT

Pollution of water sources is a growing problem in modern society, with dyes from the textile and manufacturing industry being one of the most common pollutants in wastewater. The improper disposal of water with residual dyes represents a risk of contamination of effluents, fresh water sources and soil. The identification of approaches to treat dyes wastewater is a need. Carbon nanomaterials, especially graphene oxide (GO) and reduced graphene oxide (rGO), are good candidates for application in filtration membranes, due to their chemical structure and physical properties. In this study, we described the production and characterization of rGO dispersions with suitable properties for the application in filtration membranes production. A facile spray coating method was employed to deposit rGO on cellulose acetate membranes, producing uniform and stable rGO filtration membranes. The thickness of deposited rGO layer varies from 0.25 to 0.72 μm, the rejection to aniline blue reached 70% and the pure water flux was 26.5 L/m^2·h, indicating that these membranes has good application prospects for dyes removal. Our study reveals a simple, cost-effective, and scalable strategy for eliminating a large proportion of dyes from wastewater across multiple industry sectors.

Keywords: Reduced graphene oxide; Water filtration; Membranes; Dye removal; Aniline blue

1. Introduction

Dyes are one of the most common pollutants in wastewater from many different fields of industry. Improper disposal of this material can contaminate potable water source and soil, causing damage to humans, animals and the environment. Since dyes may present potential biological toxicity, teratogenicity, carcinogenicity, and mutagenicity, it is essential to remove them from wastewater with effective methods [1–3].

There are many methods of dyes removal, with different characteristics and aspects. Coagulation is an important technique, because it is efficient and simple, being able to remove 88% to 96% of insoluble dyes from water. For soluble dyes, this method has limited effect, what is a disadvantage [4]. Biodegradation is a simple and inexpensive method that can completely mineralize pollutants, but this procedure alone may not be sufficient to remove non-biodegradable components from dyes [5]. Activated carbon absorption technique is also effective in dyes

* Corresponding author.

removal from water, mainly from textile industry. Despite this, commercial activated carbons can be expensive, which makes the development of activated carbons from cheap sources a goal [6,7].

The membrane separation technique stands out in relation to other procedures, mainly due to its continuous separation process, high degree of treatment, cost-effectiveness, ability to remove pollutants with different sizes and simplicity [8]. Nawaz et al. [9] studied a novel polyaniline (PANI)/polyvinylidene fluoride (PVDF) hybrid membrane and achieved 85% dye rejection. Zhao et al. [10] produced a nanofiltration membrane with layered double hydroxides/polymer and also obtained high rejection for dyes (methyl blue 97.9% and acid fuchsin 97.5%)

Graphene oxide (GO) and reduced graphene oxide (rGO) are good candidates for producing composite membranes for water purification, as the capillary effect generated by stacked nanosheets increases both water flux and solute rejection [1]. Some characteristics of these materials are crucial for this application, such as flexibility, hydrophilicity, good mechanical strength, low-cost production and the possibility of production in large scale [11].

Fan et al. [12] compared GO and rGO membranes for dyes removal and concluded that the rGO membranes exhibited better stability, high water permeance and rejection. Qiu et al. [13] concluded that reduction temperature of rGO membranes could affect the permeation properties for nanofiltration. Zhang et al. [14] studied rGO membranes and obtained 56.3 L/m²·h·bar of water permeance and high rejection over 95% for various dyes. Sheng et al. [15] prepared rGO composite membranes for catalytic oxidation of sulfamethoxazole and confirmed the potential of these membranes for practical applications in water purification. Pei et al. [16] obtained faster permeation in rGO membranes, compared to those produced with pristine graphene oxide, revealing the potential of using graphene-based membranes in desalination and water treatment.

In this work, a simple, original and fast method to remove dyes from wastewater with rGO-based sprayed filtration membranes was demonstrated, which can be scaled-up for water treatment in paper, cosmetics, plastics, printing and textile industries. Morphology and composition of rGO membranes were evaluated by X-ray diffraction, Raman spectroscopy and scanning electron microscopy. Pure water flux, hydrophilicity and dye rejection were also studied.

2. Materials and methods

2.1. Preparation of rGO dispersions

Modified Hummers method [17,18] was applied to produce GO dispersion, promoting intercalation and oxidation for 7 d, by adding 10 g of graphite flakes to 7.6 g of sodium nitrate ($NaNO_3$), 338 mL of sulfuric acid (H_2SO_4) and 49.5 g of potassium permanganate ($KMnO_4$), followed by exfoliation with 12 washing/centrifugation steps with sulfuric acid and hydrogen solution (3% H_2SO_4 0.5% H_2O_2) plus 5 centrifugation steps with distilled water.

GO was reduced by adding ascorbic acid as reducing agent, ammonium hydroxide (NH_4OH) and polystyrene sulfonate (PSS), the mixture was stirred using a magnetic plate for 35 min. After this step, the material was placed in an oven and heated at 80°C for 3 d, followed by 5 washing/centrifugation steps with distilled water in order to eliminate excess reagents, producing rGO dispersions.

2.2. Preparation of rGO filtration membranes

Cellulose acetate (CA) membranes from UNIFIL (Brazil), with 0.2 μm of pore size and 25 mm of diameter, were used as substrate to deposit graphene. rGO dispersions were elected to produce filtration membranes (FM) because this material presents less oxygen-containing functional groups, which improves membrane permeability and stability, without sacrificing rejection [10]. rGO FM were produced by spray coating method (Steula BC-66-08 airbrush with nozzle of 0.8 mm). The following parameters were used: 1.0 mg/mL rGO dispersions, 20 psi of nitrogen as carrier gas, membrane temperature of 90°C (heated with a hot plate), 1 s time of coating deposition, 30 s of drying time between depositions and variable numbers of coatings: 40 (named as 40-coat. rGO FM), 60 (60-coat. rGO FM), 80 (80-coat. rGO FM) and 100 (100-coat. rGO FM).

2.3. Characterization

GO and rGO dispersions were characterized by X-ray photoelectron spectroscopy (XPS), by SPECS 100 equipment, using a double Al-Kα radiation source, 2-DLine detector and scanning with initial energy from 1,280 to 20 eV. The data obtained were later processed with the help of the CasaXPS software. rGO flakes were analyzed by scanning electron microscopy (SEM) in QUANTA FEG FEI equipment, with magnifications ranging from 500× to 1,000×, voltage of 2 kV, spot size 4.5 to 5.0 and working distance from 4.7 to 8.3 mm. The lateral dimension of rGO flakes was obtained by measuring with xT microscope control software help.

Chemical and morphological characterizations of filtration membranes were obtained by the following techniques: X-ray diffraction (XRD), with a X'Pert MRD PANalytical equipment, cobalt source, 40 kV and 40 mA of voltage and current; Raman spectroscopy, with a home-built spectrometer from Interfaces Laboratory of CBPF with a laser of 488 nm and 180 s of radiation time and SEM, also in QUANTA FEG FEI, with voltage of 5 kV, spot size 3 to 5 and working distance from 11.5 to 14.4 mm. All samples were analyzed to verify if there would be any contamination or other problem in deposition method. For cross-section images, the samples were cryo-snapped with liquid nitrogen [15] and analyzed with a JEOL (JSM 7100F, Japan) SEM equipment, using voltage of 5 kV.

Stability was observed by soaking the membranes in deionized water for 5, 15 and 30 d. Hydrophilicity and the permeate flux were also evaluated. An analysis of the contact angle was performed with an FTA100 goniometer, taking three measurements of a deionized water drop with 0.2 μL in each surface membrane at room temperature.

Pure water flux was evaluated by a home-made permeation cell (Fig. 1), with 2 bar of N_2. Before analysis, membranes were pre-pressurized during 1 h, until water permeance reached a stable value. The water flux was calculated using Eq. (1), where Q (L) is the volume of permeation,

A (m^2) is the effective area analyzed and Δt (h) is the permeation time [19,20].

$$J_w = \frac{Q}{A \cdot \Delta t} \qquad (1)$$

2.4. Evaluation of dye removal

The capability of dye removal of rGO filtration membranes was evaluated using the same home-made permeation cell (Fig. 1), also with 2 bar of N$_2$. Pre-pressuring procedure for 1 h was also applied. CA pure membrane and rGO filtration membranes with 40, 60, 80 and 100 coatings were tested. 20 ppm aniline blue aqueous solution was used as feed solution, simulating a dye wastewater.

UV-Vis absorption spectra of feed and permeation solution were made with CARY 5000 spectrophotometer, from VARIAN. The analyses were obtained for wavelengths from 400 to 700 nm. A standard curve in 578 nm (where the aniline blue absorption peak was found experimentally) was performed and used to obtain dye concentration in ppm. The rejections (R) were calculated using Eq. (2), where C_v is the concentration of the permeate and C_f is the feed solution concentration [20–22].

$$R = \left(1 - \frac{C_p}{C_f}\right) \times 100\% \qquad (2)$$

3. Results and discussion

3.1. rGO dispersion characterization

Fig. 2 exhibits the XPS spectra of GO and rGO dispersions. It is possible to note the presence of sodium (Na 1s), oxygen (O 1s), carbon (C 1s) and sulfur (S 2p) in rGO sample.

Comparing the atomic percentage values obtained between the reduced and non-reduced samples, it is observed that the reduction process was effective, given the oxygen decrease (37% to 24%) and carbon increase (58% to 69%) in the rGO sample in relation to GO. GO reduction can also be confirmed by C/O ratio: 1.58 for GO and 2.83 for rGO.

SEM micrographs for rGO flakes can be observed in Fig. 3. It is possible to notice morphological characteristics compatible with rGO, such as thin sheets and folds. The lateral dimensions of flakes were also studied, 50 flakes were measured reaching an average value of 45.9 ± 26.6 μm; this dimension is very appropriate since large GO and rGO sheet sizes can direct affect permeability, salt rejection and other aspects. For example, large graphene sheets are more successful in eliminate salt from water then medium and small sizes [23].

3.2. rGO filtration membranes characterization

As evidenced from XRD diffractograms in Fig. 4, CA membrane presents an amorphous halo at 2θ = 7.2° and rGO filtration membranes have a peak at 2θ = 7.8°, which are related to (002) crystal plane of GO [24–26], which means that the rGO employed was partially reduced. Above 60 coatings, the characteristic peak of GO became more intense.

Raman spectra for the CA membrane and rGO filtration membranes can be observed in Fig. 5. It is possible to note elevations in the Raman shift correlated to the D (1,361 cm^{-1}) and G (1,595 cm^{-1}) bands, which are related to structural defects and to the sp^2 carbon domains, respectively, being D band the one that identifies the structure of graphene, confirming that the deposition method was efficient [26].

The 2D band is presented at 2,701 cm^{-1} of all spectra and is related to the intensity of the number of graphene layers [27].
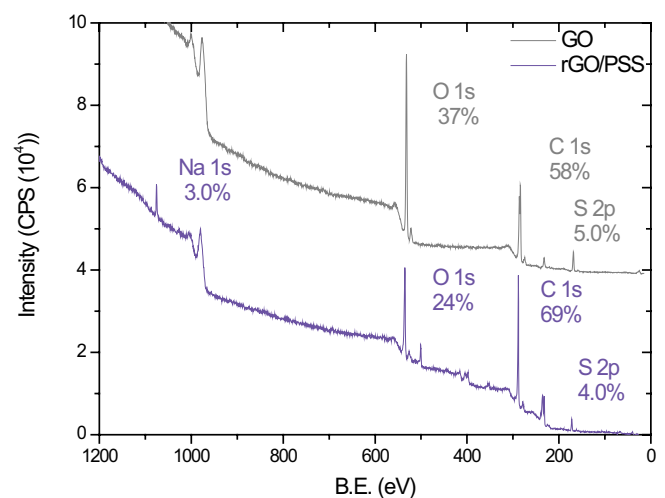

Fig. 1. Permeation cell.

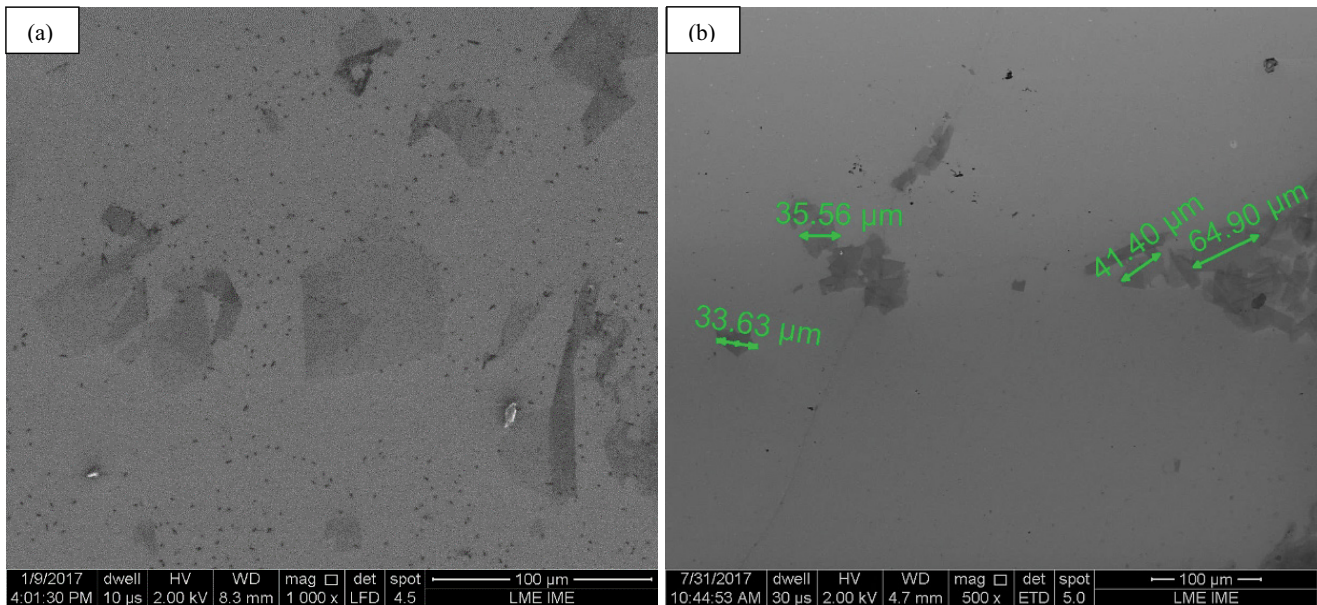Fig. 2. XPS spectra of GO and rGO dispersions.

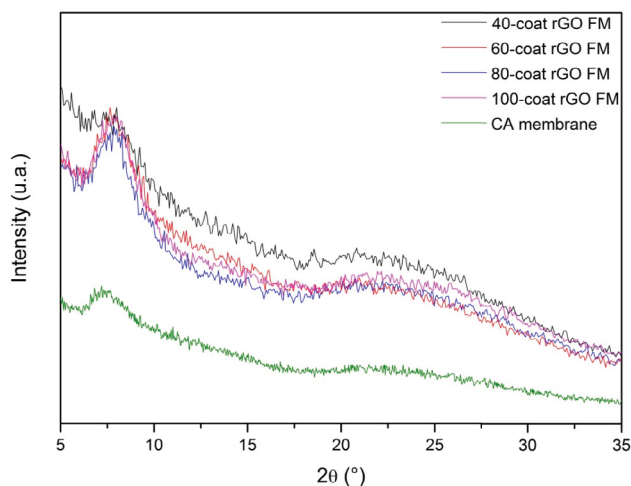Fig. 3. SEM micrographs for (a) rGO and (b) rGO with dimension measurements.

Fig. 4. XRD patterns for CA membrane and rGO filtration membranes (FM) with different number of coatings (coat.).

Fig. 5. Raman spectra of CA membrane and rGO FM.

At 2,958 cm^{-1}, D + G band is identified, which is activated by defects [28]. The CA membrane practically does not have bands in comparison with rGO filtration membranes.

SEM micrographs (Fig. 6) also indicated that the spray coating method was efficient in deposit graphene flakes on membrane surface. In Fig. 6a it is possible to observe the uniform surface with pores from the commercial CA membrane, whereas in as-prepared rGO filtration membranes samples (Fig. 6b–e) the micrographs acquire a rough aspect, characteristic from an accumulation of graphene, with plenty of wrinkles and without visible defects.

Fig. 7 displays the cross-sectional SEM images for all membranes in this study and their respective rGO deposited thickness. It is possible to observe that the thickness of the rGO layer varies from 0.25 to 0.72 µm and increases, reciprocally, with the amount of layers deposited over the pure
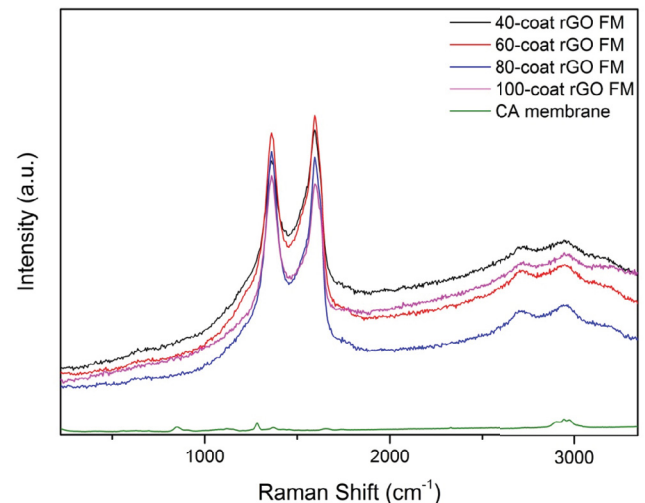
membrane. This corroborates that the spray coating method is suitable for the production of rGO filtration membranes and also that the thickness of rGO layer does not affect the surface morphology.

3.3. Membrane stability, permeate flux and hydrophilicity

Hydrated membranes remained stable and intact during at least 30 d immersed in water. The stability could be attributed to the balance between van der Waals forces and repulsive hydration of graphene [29]. This interlayer stability achieved with the spray technique represents great significance for filtration applications.

Pure water flux and the contact angle of different rGO FM are presented in Fig. 8. The flux values of 40-coat. rGO FM, 60-coat. rGO FM, 80-coat. rGO FM and 100-coat. rGO
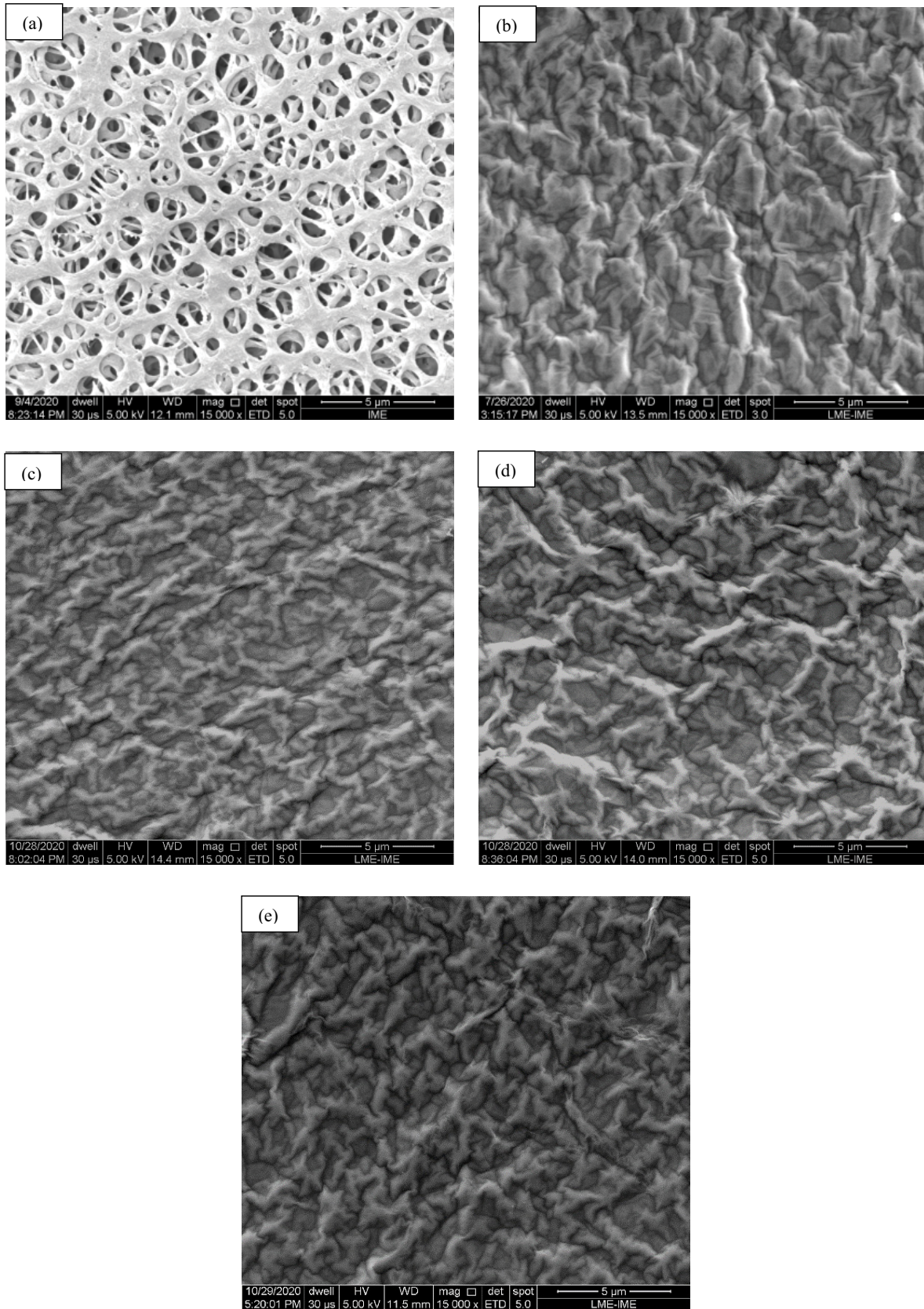
Fig. 6. SEM micrographs for: (a) CA membrane, (b) 40-coat. rGO FM, (c) 60-coat. rGO FM, (d) 80-coat. rGO FM, and (e) 100-coat. rGO FM.
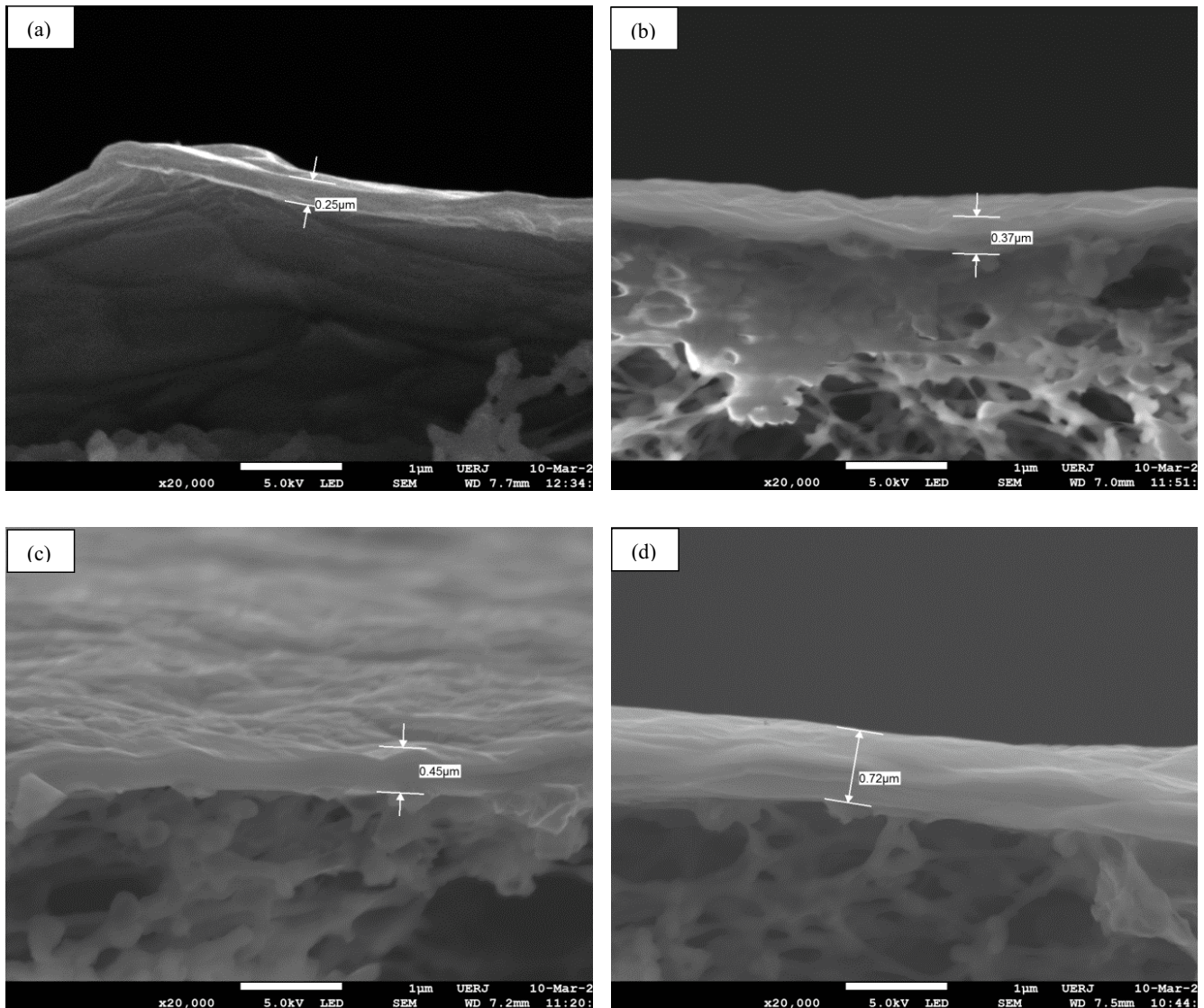
Fig. 7. Cross-sectional SEM micrographs for: (a) 40-coat. rGO FM, (b) 60-coat. rGO FM, (c) 80-coat. rGO FM, and (d) 100-coat. rGO FM.

FM were 20.35 ± 10.7, 10.68 ± 4.7, 15.49 ± 7.3 and 8.8 ± 4.6 L/m^2·h, respectively. The highest water flux was exhibited by 40-coat. rGO FM and the lowest by 100-coat. rGO FM, which is related to the membrane thickness and possibly, the presence of longer channels for water passage, resulting in increased of the transport resistance [12]. These results are in agreement with the values obtained by other authors, for GO and rGO filtration membranes, produced with more complex and laborious techniques [12,25,29].

The contact angles of the studied filtration membranes are between 17° and 30°, the hydrophilic character of the membranes also supports the hypothesis that rGO was partially reduced, therefore, the residual oxygen-containing functional groups are responsible for this behavior. Composite membranes which exhibit hydrophilic surfaces can provide a fast channel for the passage of water molecules [30]. So, the membrane with the highest water flow is the one presenting the lowest contact angle, as shown in Fig. 8.

3.4. Dye removal evaluation

The aspect of CA membrane and rGO filtration membranes, before and after permeation test, can be seen in Fig. 9. It is possible to observe that the analyzed area of all rGO FM did not suffer significant damage during tests, indicating that the studied membranes are stable in water flux.

The UV-Vis absorption spectra of feed and permeated solutions can be seen in Fig. 10. Analyzing the curves, it is possible to notice that the CA membrane has the ability to filter out some part of the dye, but not a significant amount. By absorption spectra analysis, it is also possible to indicate that most of the dye was successfully eliminated from the feed solution in samples with 40, 60 and 80 coatings of rGO deposited on the CA membrane.

The permeated solution of the filtration membrane with 100 layers of rGO presented a light brown color, which may indicate that some part of the graphene detached off the membrane, mixing to the permeated water, even though the

membrane appearance (Fig. 9j) did not exhibit a significant failure in rGO film surface. It could indicate that 100 coatings of deposited rGO can be excessive and prejudicial to the filtration process.

Dye rejection is show in Fig. 11, which is an important parameter for membrane performance [1]. It is possible to notice an increase of about 15% in the rejection capacity of membranes with rGO (72%), compared to the pure CA membrane (57%). These results are slightly below those obtained in other studies (74% and 88% of rejection for methyl orange and methylene blue in GO membranes [1], 96% for methyl blue also in GO membranes [22], 99% for methyl blue in rGO membranes [12] and 99.7% for methylene blue in MWCNTs-COOH intercalated GO membranes [34]); but the spray method employed in the present work has the advantage of being a faster and simpler production process, with the possibility of scalability for the industry [31–33].
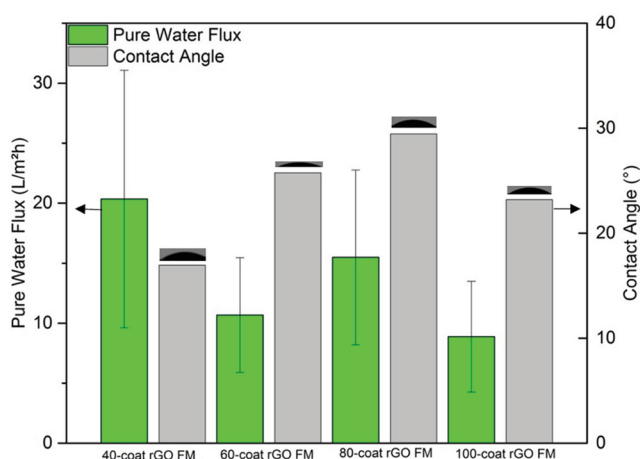
The increase in the number of rGO film coatings deposited did not affect the rejection rate, which indicates that only 40 coatings of deposited film present satisfactory results, making the process faster and economical. The 100-ly rGO FM rejection results were impacted by the material detachment during analyses.

4. Conclusions

In summary, an effective strategy to produce rGO filtration membranes was described in detail. rGO dispersion was successfully reduced, and rGO flakes presents lateral size and properties suitable for production of filtration membranes. Various methods were employed to characterize the rGO membranes, and the results indicate that the spray coating method was capable to produce

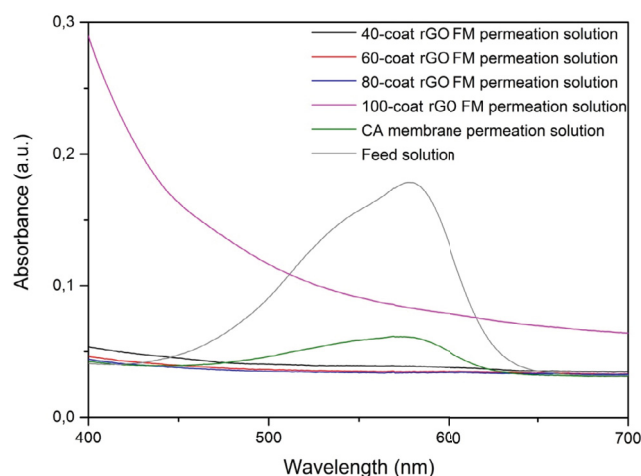Fig. 8. Pure water flux and contact angle for rGO FM.

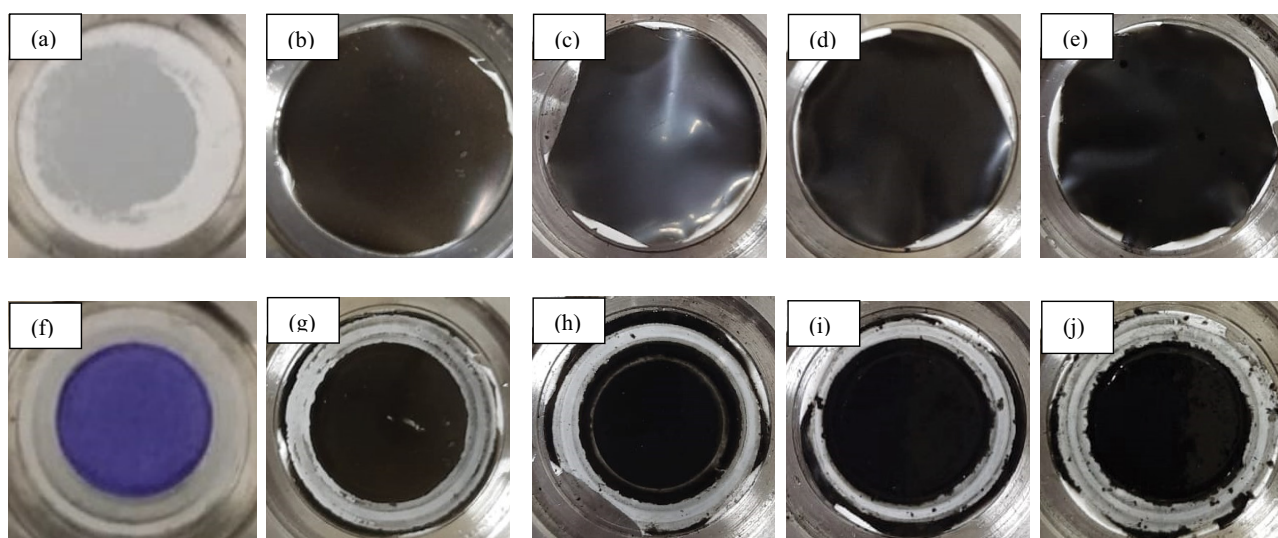Fig. 10. UV-Vis absorption spectra for feed and permeated solutions.

Fig. 9. Filtration membranes: (a) CA membrane, (b) 40-coat. rGO FM, (c) 60-coat. rGO FM, (d) 80-coat. rGO FM, (e) 100-coat. rGO FM before permeation test, (f) CA membrane, (g) 40-coat. rGO FM, (h) 60-coat. rGO FM, (i) 80-coat. rGO FM, and (j) 100-coat. rGO FM after permeation test.
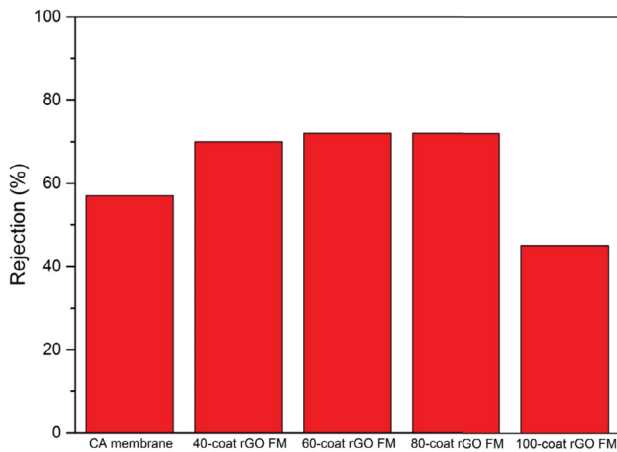
Fig. 11. Dye rejection of CA membrane and rGO FM.

uniform, uncontaminated and stable membranes. The efficiency of the produced membranes was evaluated through the permeation test, which proved that the resulting membrane has a fast pure water flow (26.5 L/m²·h) and a good retention rate (70%). This works provides a simple, low-cost and scalable strategy to remove most part of aniline blue from manufacturing and textile industry wastewater.

Acknowledgments

Symbols

J_w	—	Water flux, L/m²·h
Q	—	Volume of permeation, L
A	—	Effective area, m²
Δt	—	Permeation time, h
R	—	Rejections, %
C_p	—	Permeate solution concentration, ppm
C_f	—	Feed solution concentration, ppm

References

[1] X. Yan, W. Tao, S. Cheng, C. Ma, Y. Zhang, Y. Sun, X. Kong, Layer-by-layer assembly of bio-inspired borate/graphene oxide membranes for dye removal, Chemosphere, 256 (2020) 127118–127127.

[2] J. Li, J.L. Gong, G.M. Zeng, P. Zhang, B. Song, W.C. Cao, S.Y. Fang, S.Y. Huan, J. Ye, The performance of UiO-66-NH₂/graphene oxide (GO) composite membrane for removal of differently charged mixed dyes, Chemosphere, 237 (2019) 124517–124530.

[3] S. Ariaeenejad, E. Motamedi, G.H. Salekdeh, Application of the immobilized enzyme on magnetic graphene oxide nano-carrier as a versatile bi-functional tool for efficient removal of dye from water, Bioresour. Technol., 319 (2021) 124228–124237.

[4] X. Huang, Y. Wan, B. Shi, J. Shi, H. Chen, H. Liang, Characterization and application of poly-ferric-titanium-silicate-sulfate in disperse and reactive dye wastewaters treatment, Chemosphere, 249 (2020) 126129–126139.

[5] M. Rajasimman, S.V. Babu, N. Rajamohan, Biodegradation of textile dyeing industry wastewater using modified anaerobic sequential batch reactor – start-up, parameter optimization and performance analysis, J. Taiwan Inst. Chem. Eng., 72 (2017) 171–181.

[6] C.S. Lin, K.L. Tung, Y.L. Lin, C.D. Dong, C.W. Chen, C.H. Wu, Fabrication and modification of forward osmosis membranes by using graphene oxide for dye rejection and sludge concentration, Process Saf. Environ. Prot., 144 (2020) 225–235.

[7] S. Wong, N. Ngadi, I.M. Inuwa, O. Hassan, Recent advances in applications of activated carbon from biowaste for wastewater treatment: a short review, J. Cleaner Prod., 175 (2018) 361–375.

[8] H. Zeng, Z. Yu, L. Shao, X. Li, M. Zhu, Y. Liu, X. Feng, X. Zhu, Ag₂CO₃@UiO-66-NH₂ embedding graphene oxide sheets photocatalytic membrane for enhancing the removal performance of Cr(VI) and dyes based on filtration, Desalination, 491 (2020) 114558–114569.

[9] H. Nawaz, M. Umar, I. Nawaz, A. Ullah, M. Khawar, M. Nikiel, H. Razzaq, M. Siddiq, X. Liu, Hybrid PVDF/PANI membrane for removal of dyes from textile wastewater, Adv. Eng. Mater., 24 (2022) 2100719–2100730.

[10] S. Zhao, H. Zhu, Z. Wang, P. Song, M. Ban, X. Song, A loose hybrid nanofiltration membrane fabricated via chelating-assisted in-situ growth of Co/Ni LDHs for dye wastewater treatment, Chem. Eng. J., 353 (2018) 460–471.

[11] T. Wang, J. Lu, L. Mao, Z. Wang, Electric field assisted layer-by-layer assembly of graphene oxide containing nanofiltration membrane, J. Membr. Sci., 515 (2016) 125–133.

[12] X. Fan, C. Cai, J. Gao, X. Han, J. Li, Hydrothermal reduced graphene oxide membranes for dyes removing, Sep. Purif. Technol., 241 (2020) 116730–116738.

[13] L. Qiu, X. Zhang, W. Yang, Y. Wang, G.P. Simon, D. Li, Controllable corrugation of chemically converted graphene sheets in water and potential application for nanofiltration, Chem. Commun., 47 (2011) 5810–5812.

[14] Q. Zhang, X. Qian, K.H. Thebo, H.M. Cheng, W. Ren, Controlling reduction degree of graphene oxide membranes for improved water permeance, Sci. Bull., 63 (2018) 788–794.

[15] J. Sheng, H. Yin, F. Qian, H. Huang, S. Gao, J. Wang, Reduced graphene oxide-based composite membranes for in-situ catalytic oxidation of sulfamethoxazole operated in membrane filtration, Sep. Purif. Technol., 236 (2020) 116275–116284.

[16] J. Pei, X. Zhang, L. Huang, H. Jiang, X. Hu, Fabrication of reduced graphene oxide membranes for highly efficient water desalination, RSC Adv., 6 (2016) 101948–101953.

[17] J.P. Rourke, P.A. Pandey, J.J. Moore, M. Bates, I.A. Kinloch, R.J. Young, N.R. Wilson, The real graphene oxide revealed: stripping the oxidative debris from the graphene-like sheets, Angew. Chem. Int. Ed., 50 (2011) 3173–3177.

[18] W.S. Hummers, R.E. Offeman, Preparation of graphitic oxide, J. Am. Chem. Soc., 80 (1958) 1339, doi: 10.1021/ja01539a017.

[19] J. Hou, Y. Chen, W. Shi, C. Bao, X. Hu, Graphene oxide/methylene blue composite membrane for dyes separation: formation mechanism and separation performance, Appl. Surf. Sci., 505 (2020) 144145–144157.

[20] S.P. Sundaran, C.R. Reshmi, P. Sagitha, O. Manaf, A. Sujith, Multifunctional graphene oxide loaded nanofibrous membrane for removal of dyes and coliform from water, J. Environ. Manage., 240 (2019) 494–503.

[21] N.C. Homem, N.C.L. Beluci, S. Amorim, R. Reis, A.M.S. Vieira, M.F. Vieira, R. Bergamasco, M.T.P. Amorim, Surface modification of a polyethersulfone microfiltration membrane with graphene oxide for reactive dyes removal, Appl. Surf. Sci., 486 (2019) 499–507.

[22] N. Mehrabi, H. Lin, N. Aich, Deep eutectic solvent functionalized graphene oxide nanofiltration membranes with superior water permeance and dye desalination performance, Chem. Eng. J., 412 (2021) 128577–128588.

[23] A. Gogoi, T.J. Konch, K. Raidongia, K.A. Reddy, Water and salt dynamics in multilayer graphene oxide (GO) membrane: role of lateral sheet dimensions, J. Membr. Sci., 563 (2018) 785–793.

[24] J. Li, M. Hu, H. Pei, X. Ma, F. Yan, D.S. Dlamini, Z. Cui, B. He, J. Li, H. Matsuyama, Improved water permeability and structural stability in a polysulfone-grafted oxide composite membrane used for dye separation, J. Membr. Sci., 595 (2020) 117547–117558.

[25] R. Zhang, Y. Ma, W. Lan, D.E. Sameen, S. Ahmed, J. Dai, W. Qin, S. Li, Y. Liu, Enhanced photocatalytic degradation of organic dyes by ultrasonic-assisted electrospray TiO_2/graphene oxide on polyacrylonitrile/β-cyclodextrin nanofibrous membranes, Ultrason. Sonochem., 70 (2021) 105343–105361.

[26] A. Hassanpour, S. Nahar, X. Tong, G. Zhang, M.A. Gauthier, S. Sun, Photocatalytic interlayer spacing adjustment of a graphene oxide/zinc oxide hybrid membrane for efficient water filtration, Desalination, 475 (2020) 114174–114182.

[27] H. Xu, L. Ma, Z. Jin, Nitrogen-doped graphene: synthesis, characterizations and energy applications, J. Energy Chem., 27 (2018) 146–160.

[28] K.K.H de Silva, H.H. Huang, M. Yoshimura, Progress of reduction of graphene oxide by ascorbic acid, Appl. Surf. Sci., 447 (2018) 338–346.

[29] J. Ma, X. Tang, Y. He, Y. Fan, J. Chen, HaoYu, Robust stable MoS_2/GO filtration membrane for effective removal of dyes and salts from water with enhanced permeability, Desalination, 480 (2020) 114328–114338.

[30] M. Zhu, Y. Liu, M. Chen, D. Gan, M. Wang, H. Zeng, M. Liao, J. Chen, W. Tu, W. Niu, Ultrahigh flux of graphene oxide membrane modified with orientated growth of MOFs for rejection of dyes and oil-water separation, Chin. Chem. Lett., 31 (2020) 2683–2688.

[31] A. Morelos-Gomez, R. Cruz-Silva, H. Muramatsu, J. Ortiz-Medina, T. Araki, T. Fukuyo, S. Tejima, K. Takeuchi, T. Hayashi, M. Terrones, M. Endo, Effective NaCl and dye rejection of hybrid graphene oxide/graphene layered membranes, Nat. Nanotechnol., 12 (2017) 1083–1088.

[32] P. Liu, C. Zhu, A.P. Mathew, Mechanically robust high flux graphene oxide – nanocellulose membranes for dye removal from water, J. Hazard. Mater., 371 (2019) 484–493.

[33] M. Khansanami, A. Esfandiar, High flux and complete dyes removal from water by reduced graphene oxide laminate on poly vinylidene fluoride/graphene oxide membranes, Environ. Res., 201 (2021) 111576–111585.

[34] W. Zeng, C. Li, Y. Feng, S. Zeng, B. Fu, X. Zhang, Carboxylated multi-walled carbon nanotubes (MWCNTs-COOH)-intercalated graphene oxide membranes for highly efficient treatment of organic wastewater, J. Water Process Eng., 40 (2021) 101901–101909.